Supporting Information

Critical Role of *Chlamydomonas reinhardtii* Ferredoxin-5 in Maintaining Membrane Structure and Dark Metabolism

Wenqiang Yang[a,1,2], Tyler M. Wittkopp[a, b,1], Xiaobo Li[a], Jaruswan Warakanont[c], Alexandra Dubini[d], Claudia Catalanotti[a], Rick G. Kim[a,b], Eva C. M. Nowack[a], Luke C.M. Mackinder[a], Munevver Aksoy[a], Mark Dudley Page[e], Sarah D'Adamo[f], Shai Saroussi[a], Mark Heinnickel[a], Xenie Johnson[a,g], Pierre Richaud[g], Jean Alric[a,g], Marko Boehm[d], Martin C. Jonikas[a], Christoph Benning[h], Sabeeha S. Merchant[e,i], Matthew C. Posewitz[f], Arthur R. Grossman[a]

[1] *W.Y. and T.M.W. contributed equally to this work.*

[a] Department of Plant Biology, Carnegie Institution for Science, Stanford, CA 94305, USA

[b] Department of Biology, Stanford University, Stanford, CA 94305, USA

[c] Department of Plant Biology, Michigan State University, East Lansing, MI 48824, USA

[d] National Renewable Energy Laboratory, Golden, CO 80401, USA

[e] Department of Chemistry and Biochemistry, University of California, Los Angeles, CA 90095, USA

[f] Department of Chemistry and Geochemistry, Colorado School of Mines, Golden, CO 80401, USA

[g] Commissariat à l'Énergie Atomique, Centre National de la Recherche Scientifique, Aix-Marseille Université, Cadarache, Saint-Paul-lez-Durance, F-13108, France

[h] MSU-DOE-Plant Research Laboratory, Michigan State University, East Lansing, MI 48824

[i] Institute of Genomics and Proteomics, University of California, Los Angeles, CA 90095, USA

[2] *To whom correspondence should be addressed. Email: wenqiangy@gmail.com*

SI APPENDIX

SI Materials and Methods

Southern Blot analysis

Genomic DNA (gDNA) was isolated and purified using a standard phenol-chloroform extraction from 50 ml liquid cultures, digested with various restriction enzymes and the DNA fragments resolved by agarose (0.8%) gel electrophoresis, and then blotted for 20 h in SSC onto nylon membranes (Bio-Rad, Hercules, CA). Transferred DNA was cross-linked, with hybridizations performed as previously described[1]. The *AphVIII* ORF (805 bp) and *FDX5*-specific DNA fragments (315 bp) were amplified with primers APH8-F1/APH8-R1 and FDX5-F4/ FDX5-R4 (see ***SI Appendix*, Table S2**) and used as hybridization probes. To visualize hybridizing bands, blots were exposed to a phosphor screen (Molecular Dynamics) and imaged using a Pharos FX Plus scanner with Quantity One software (Bio-Rad).

pLM005_Venus constructs and transformation

The *FDX5*, *CrΔ4FAD* and *CrFAD6* genes were amplified from cDNAs and cloned into pLM005_Venus by Gibson assembly cloning[2,3] to generate pLM005FDX5_Venus, pLM005CrΔ4FAD_Venus, and pLM005CrFAD6_Venus with various regulatory regions, as noted in the text. The constructs were transformed into cMJ030 (CC-4533) and transformants identified based on fluorescence outputs of individual colonies, and localized as previously described[2,4].

Thylakoid membrane purification

Cells were grown to exponential phase in the light and dark and thylakoids purified as previously described[5].

Membrane inlet mass spectrometry (MIMS)

MIMS was used to differentiate between O_2 consumption and evolution in the light[6]. WT and mutant cell suspensions were equilibrated with equimolar concentrations of $^{18}O_2$ and $^{16}O_2$. Dark respiration was measured for 1-2 min prior to illuminating samples with white actinic light (~500 µmol photons m^{-2} s^{-1}); O_2 evolution and consumption were calculated as previously described[6].

In vivo photosynthetic measurements

The quantum yield of PSII (ΦPSII; F_v/F_m) and electron transport rates (ETR) were determined using a Walz DUAL-PAM 100 fluorometer, as described by the manufacturer.

Chlorophyll fluorescence measurements

Whole cell Chl fluorescence measurements were performed using a Bio-Logic JTS-10 spectrophotometer with and without the addition of inhibitors [10 µM 3-(3,4-dichloroprenyl)-1–1-dimethylurea (DCMU)] and electron acceptors [1 mM methyl viologen (MV)].

P700 determination

PSI was measured by monitoring absorption changes at 705 nm in the presence of PSII inhibitors (10 μM DCMU and 1 mM HA) during a brief period of illumination at 165 μmol photons m^{-2} s^{-1}. A saturating pulse was provided after 5 sec of illumination to oxidize all P700. In some cases, 1 mM methyl viologen (MV) was added as an acceptor of electrons from PSI.

Protein isolation, SDS-PAGE and immunoblot analysis

Cells were stored at -80^{o}C, prior to resolution of proteins by SDS-PAGE[7]. The resolved proteins were immunoblotted, probed with specific antibodies and detected using the secondary antibody horseradish peroxidase-conjugated anti-rabbit IgG (Promega, Madison, WI); peroxidase activity was detected by an enhanced chemiluminescence assay (ECL) (Amersham Biosciences, GE Healthcare, Piscataway, NJ).

Pull-Down assay

FDX5 was coupled to cyanogen bromide (CnBr)-activated sepharose beads (GE Healthcare, USA; 5 mg of protein per ml resin) and prepared according to the manufacturer's instruction. The pull-down assay was performed as described previously[8].

Mass-Spectrometry analysis

Protein samples (25 μg) were protease treated and the resulting peptides were analyzed by reverse phase chromatography using a Waters nanoAcquity UPLC pump coupled online to an LTQ/Orbitrap mass spectrometer described as previously[8] and blasted to the proteins encoded by the Chlamydomonas genome[9].

SI Appendix Figures

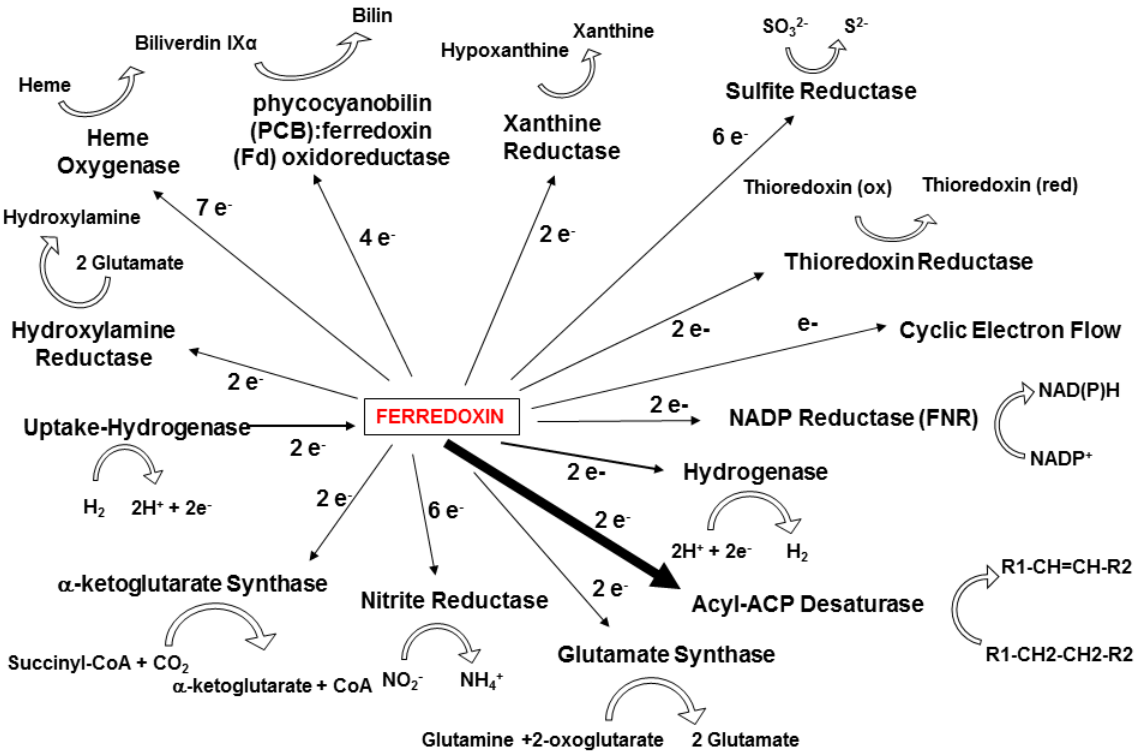

Fig. S1. Ferredoxin-mediated electron transfer reactions. Ferredoxins participate in a variety of electron transfer reactions, including those depicted; these reactions require donation of between 1 (CEF) and 7 (heme oxygenase) electrons. The transfer of electrons from ferredoxins to desaturases is highlighted by a thicker arrow since it is most relevant to the research presented.

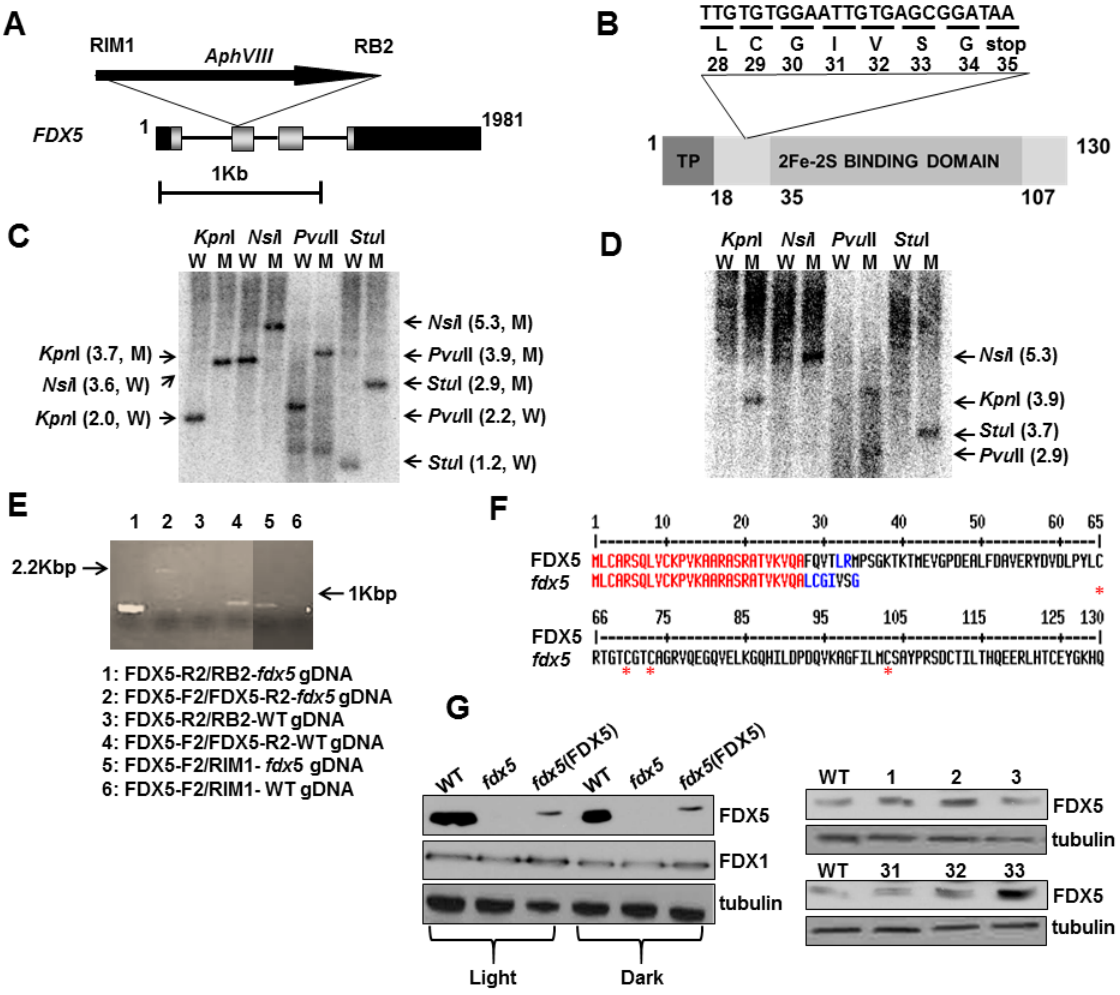

Fig. S2. Generation and molecular analyses of *fdx5* mutant. (*A*) Representation of the site of insertion of the *AphVIII* gene in the *fdx5* mutant. Black boxes represent 5' and 3'UTRs, grey boxes and black lines represent exons and introns, respectively. The arrow indicates the orientation of the insertion while the sites of primer annealing used to sequence from the cassette into the Chlamydomonas genome are designated RIM1 and RB2. (*B*) Diagram showing structure of FDX5 protein and the predicted amino acid sequence that precedes the site of translation termination of the protein in the *fdx5* mutant. TP is the chloroplast targeting transit peptide while the light grey box represents the domain that binds the 2Fe-2S cluster. The site of insertion, at amino acid 28, is indicated along with the amino acids introduced by the insertion, ending with a stop codon. (*C*) Southern blot hybridization analysis of genomic DNA from the *fdx5* mutant. The membrane with the transferred DNA was incubated with a radiolabeled probe containing the entire *FDX5* nucleotide sequence. Sizes of the hybridizing fragments are given on both sides of the blot (in Kbp). W and M represent WT and *fdx5* mutant strains, respectively. (*D*) Southern blot hybridization of genomic DNA from *fdx5* mutant using an *AphVIII* gene probe. The sizes of the hybridizing fragments are given to the right of the blot (in Kbp). (*E*) PCR with specific primers and genomic DNA (gDNA) as template was used to identify the *AphVIII* insertion site. The products generated using gDNA from WT and *fdx5* are shown. The primer pairs and templates used were: 1. FDX5-R2/RB2-*fdx5*gDNA. 2. FDX5-F2/FDX5-R2-*fdx5*gDNA. 3. FDX5-R2/RB2-WTgDNA. 4. FDX5-F2/FDX5-R2-WTgDNA. 5. FDX5-F2/RIM1-*fdx5*gDNA. 6. FDX5-F2/RIM1-WTgDNA. The fragments

amplified from the gDNA were sequenced to localize the exact insertion site. (*F*) Alignment of full-length FDX5 and the truncated FDX5 synthesized in the mutant. Note that the sequences diverge at amino acid 27 and the mutant protein is terminated at amino acid 35. The asterisks in red highlight the 4 cysteine residues involved in 2Fe-2S binding. Red represents identical amino acids between mutant and WT while the blue and black represent amino acids predicted as a consequence of the insertion. (*G*) Left panel: Western blot showing the absence of the FDX5 protein in the *fdx5* mutant [but restored in the *fdx5*(FDX5) rescued strain]. Upper panel shows abundance of FDX5, the middle panel shows the abundance of FDX1 (Fd) protein, and the lower panel shows abundance of tubulin, which was used as a loading control. Right panel: Western blot showing accumulation of FDX5 in additional *fdx5*(FDX5) rescued strains. 1, 2 and 3 represent the *fdx5*(FDX5) rescued strains from *FDX5* coding sequence (CDS), while 31, 32, 33 represent the *fdx5*(FDX5) rescued strains from *FDX5* genomic DNA. Tubulin accumulation is shown as loading controls.

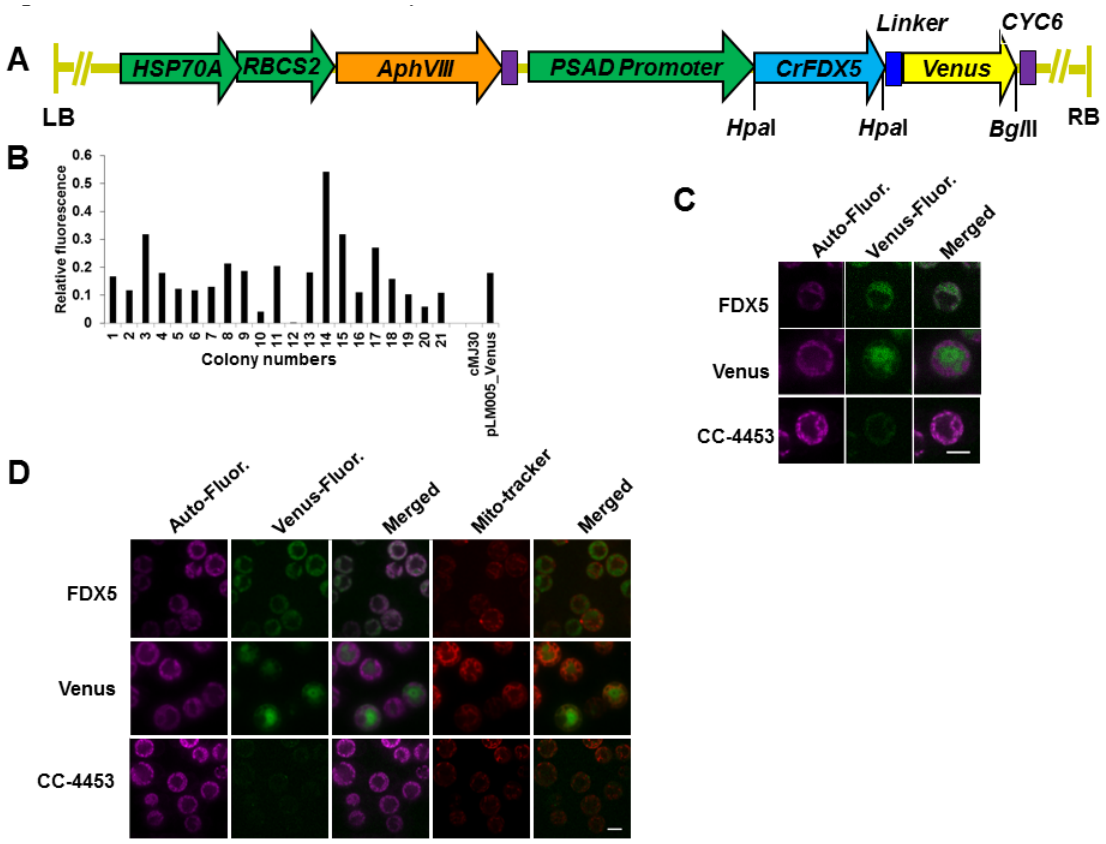

Fig. S3. FDX5 is localized to chloroplasts**.** (*A*) Schematic representation of pLM005_Venus construct containing the fusion between the *FDX5* and Venus genes. Dark green arrows represent promoters, which include the dual *HSP70* and *RBCS2* promoter driving the *AphVIII* gene (orange) and the *PSAD* (constitutive, green) promoter driving the gene encoding the FDX5-Venus fusion proteins. The *CrFDX5* gene is in blue and *Venus* in yellow. LB and RB stand for left and right border, respectively. Venus is fused to FDX5 through the linker (*35*) (dark blue) and the terminator is from CYC6 (purple. (*B*) Fluorescence was measured from the Venus-tagged Chlamydomonas transformants using a TECAN plate reader before confocal imaging of the sample was performed. Untransformed cMJ030 (CC-4533) and cMJ030 transformed with pLM005_Venus vectors (without the fusion) were used as negative and positive controls, respectively. The y-axis gives the relative fluorescence compared to the positive control (pLM005_Venus), and the x-axis represents various strains, with the rescued strains given as numbers 1-21. Fluorescence was measured 3 separate times; all replicates showed similar results. (*C*) Localization of FDX5 protein in a single Chlamydomonas cell. The cells either contained the introduced vector with neither the *Venus* nor *FDX5* sequence (CC-4533), the vector expressing *Venus* (Venus), or the vector expressing *FDX5* fused to *Venus* (FDX5-Venus). Column 1 shows Venus fluorescence (green), column 2 shows Chl autofluorescence (magenta) and column 3 shows the merged image of column 1 and column 2. The scale bar represents 5 µm. (*D*) Intracellular localization of FDX5 in Chlamydomonas. Column 1 shows Chl auto-fluorescence (magenta), column 2 shows Venus fluorescence (green), column 3 shows the merged image of column 1 and column 2, column 4 shows fluorescence of the Mito-tracker (red), and column 5 shows the merged image of column 4 and column 2. The scale bar (bottom right) represents 5 µm.

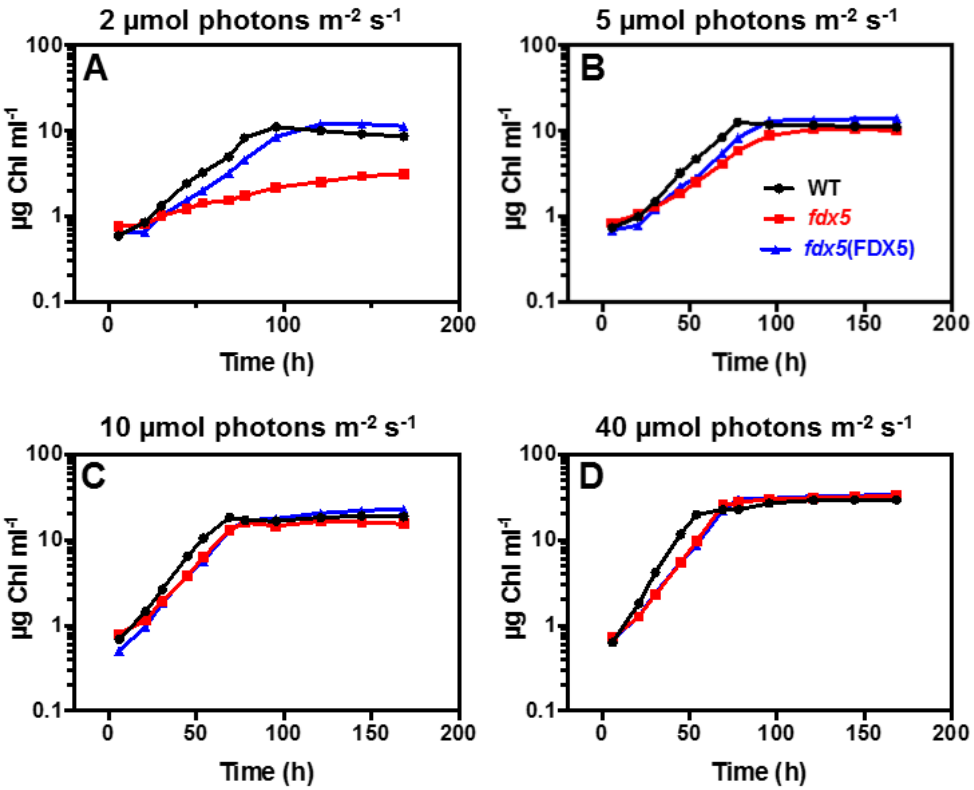

Fig. S4. *fdx5* growth at different light intensities. Growth of WT, *fdx5* and a complemented strain [*fdx5*(FDX5)] in liquid TAP medium for 7 d at 2 µmol photons m^{-2} s^{-1} (*A*), 5 µmol photons m^{-2} s^{-1} (*B*), 10 µmol photons m^{-2} s^{-1} (*C*) and 40 µmol photons m^{-2} s^{-1} (*D*). Growth was determined by measurements of Chl concentration (µg ml^{-1}), as indicated on the y-axes.

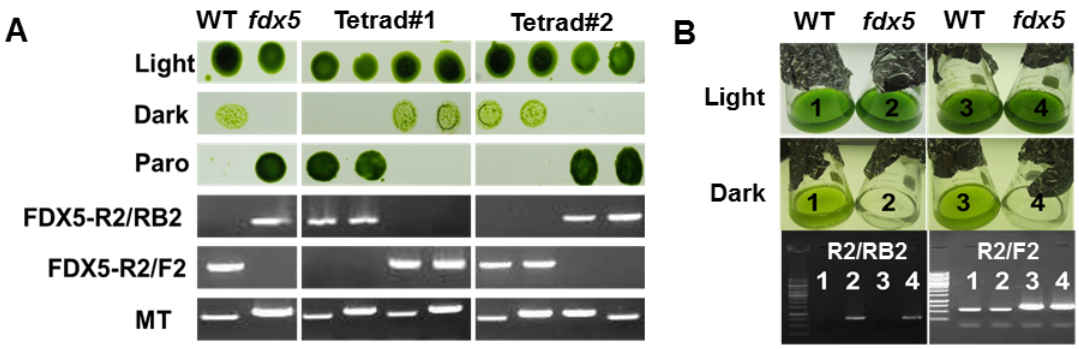

C

	P1	P2	P3	P4		P1	P2	P3	P4
Tetrad 1	*fdx5*	WT	*fdx5*	WT	Tetrad 9	*fdx5*	WT	WT	*fdx5*
Tetrad 2	WT	*fdx5*	WT	*fdx5*	Tetrad 10	*fdx5*	WT	WT	*fdx5*
Tetrad 3	WT	*fdx5*	WT	*fdx5*	Tetrad 11	*fdx5*	WT	*fdx5*	WT
Tetrad 4	WT	*fdx5*	WT	*fdx5*	Tetrad 12	WT	WT	*fdx5*	*fdx5*
Tetrad 5	*fdx5*	WT	*fdx5*	WT	Tetrad 13	WT	WT	*fdx5*	*fdx5*
Tetrad 6	WT	*fdx5*	*fdx5*	WT	Tetrad 14	*fdx5*	WT	*fdx5*	WT
Tetrad 7	WT	*fdx5*	*fdx5*	WT	Tetrad 15	*fdx5*	*fdx5*	WT	WT
Tetrad 8	*fdx5*	*fdx5*	WT	WT	Tetrad 16	WT	WT	*fdx5*	*fdx5*

Fig. S5. The *fdx5* dark growth deficiency is linked to paromomycin resistance. (*A*) Tetrad analyses: Progeny from tetrads #8 and #16 were spotted onto TAP agar (and supplemented with paromomycin), grown in the light and dark, and also inoculated into TAP liquid medium with 10 µg/ml paromomycin (Paro) and grown in the light. Liquid cultures were used for PCR to determine segregation of the *fdx5* mutation (2:2) using the FDX5-R2/RB2 primer pair (a band is amplified in the mutant but not WT progeny) or the FDX5-R2/F2 primer pair (a band is amplified in WT but not mutant progeny). PCR for mating type (MT) also exhibited 2:2 segregation. WT and the *fdx5* mutant (two leftmost columns) were used as controls. (*B*) Growth phenotype of progeny from tetrad #2; each of the progeny were grown in liquid TAP medium. 1-4 are the four daughter cells from tetrad #2, which were grown in the light or dark. PCR was performed to confirm the genotype of the progeny; the DNA from progeny 2 and 4 (the progeny unable to grow in the dark) was amplified with the FDX5-R2/RB2 primers, which only amplifies mutant DNA. (*C*) Summary of the tetrad analyses. The tetrads from 16 zygotes were analyzed by PCR. The blue and red lettering of WT and *fdx5* represent mating type + and -, respectively. P1-P4 are the four progeny of a selected tetrad.

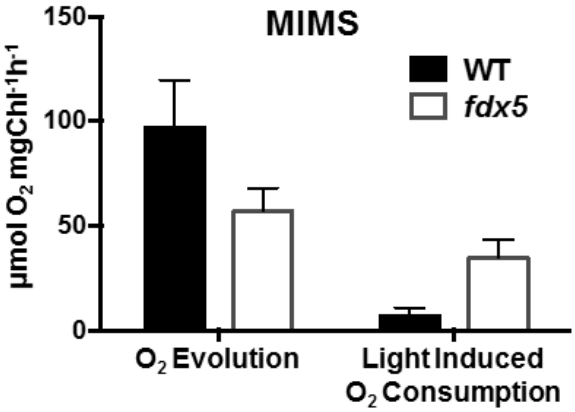

Fig. S6. Elevated light-induced O_2 consumption occurs in *fdx5* maintained in the dark. Membrane inlet mass spectrometry (MIMS analysis) was used to quantify light-induced O_2 evolution and consumption in the *fdx5* mutant and WT after 24 h in the dark. The cells used for the experiments were in mid-logarithmic phase. Error bars represent standard deviation (n=3), and the experiments were performed in triplicate.

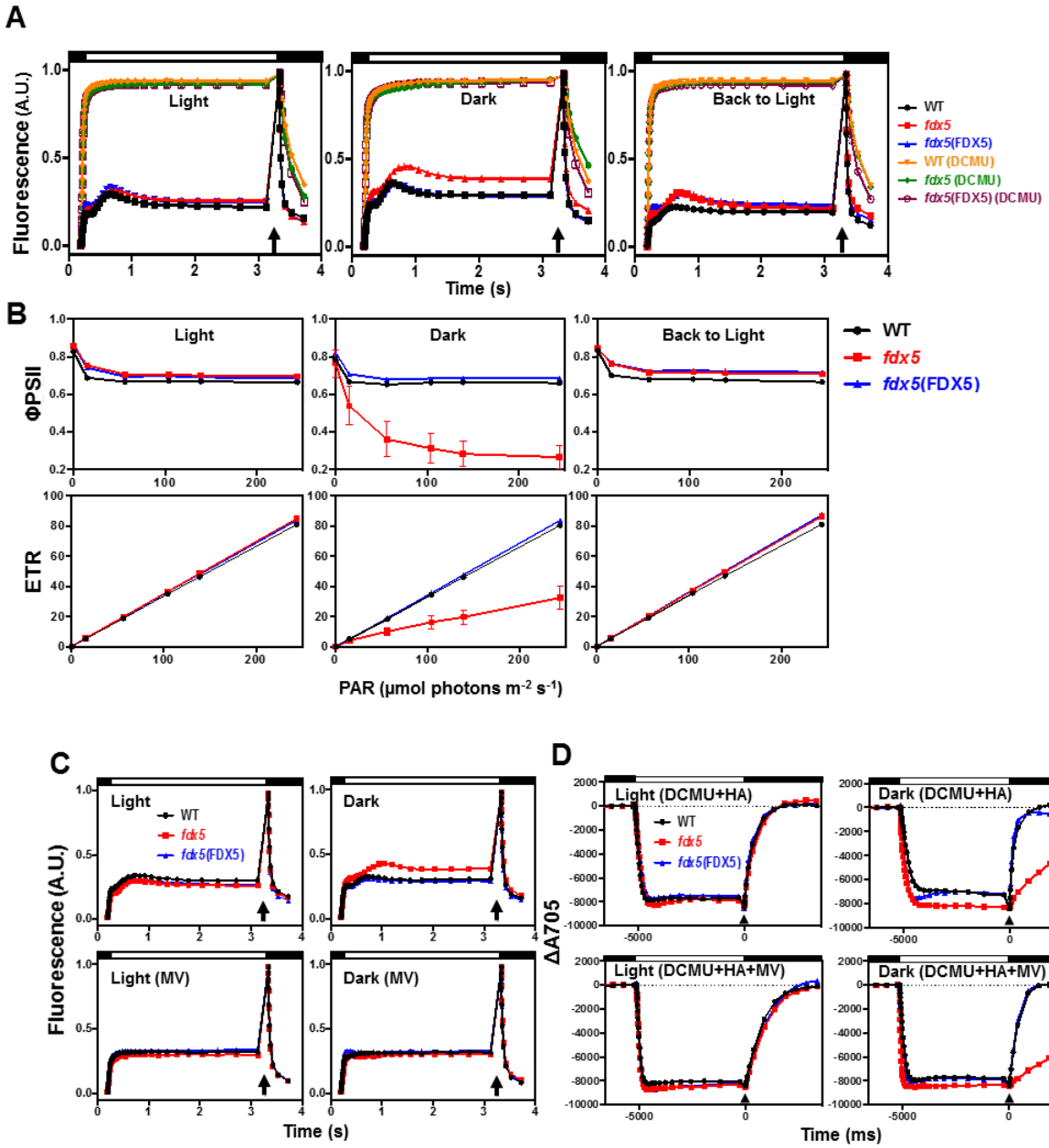

Fig. S7. Fluorescence and spectroscropic analyses show impairment of photosynthetic electron transport. (*A*) Chl fluorescence induction kinetics for cells [*fdx5* mutant, WT and the *fdx5*(FDX5) complemented strain] maintained in light or dark for 24 h, as indicated. All cells were dark-adapted for 20 min prior to the measurements. Fluorescence was measured either in the presence or absence of 3-(3,4-dichloroprenyl)-1–1-dimethylurea (10 µM) (DCMU), as indicated. The left curves show fluorescence induction for the various strains after growth in the light (**Light**); the middle curves show fluorescence induction for the various strains after maintenance in the dark for 24 h (**Dark**); the right curves show fluorescence induction after returning the dark-maintained strains to the light for 24 h (**Back to Light**). The light intensity used for the fluorescence induction curves was 156 µmol photons m^{-2} s^{-1}. (*B*) Measurement of quantum efficiency of PSII (ΦPSII) and electron transport rates (ETR) for WT, *fdx5* and the *fdx5*(FDX5) complemented strain after growth in the light (**Light**, left), maintenance in the dark for 24 h (**Dark**, middle), and maintenance in the dark for 24 h and then the dark-maintained cells transferred

back to the light for 24 h (**Back to Light**, right). Cultures were grown in TAP medium and concentrated in the same medium to 10 µg/mL Chl. All measurements were made using a DUAL-PAM 100 fluorometer. Photosynthetically Active Radiation (PAR) is given as µmol photons m^{-2} s^{-1}. Error bars represent standard deviation. (*C*) Relative Chl fluorescence measurements (using JTS-10 spectrophotometer) for WT, *fdx5* and *fdx5*(FDX5) cells grown in the light or maintained in the dark in the presence or absence of 1 mM methyl viologen (MV) as an electron acceptor, as indicated. Actinic light was on for 3 s at an intensity of 156 µmol photons m^{-2} s^{-1}. Resuspended cells were dark-adapted for 20 min prior to the measurements. (*D*) P700 oxidation-reduction kinetics on WT, *fdx5* and *fdx5*(FDX5) cells grown in the light or maintained in the dark (using JTS-10 spectrophotometer) in the presence and absence of MV. To assess the pool of electron donors to PSI, cells were resuspended in HEPES-KOH (pH 7.5, 10% Ficoll) to 30 µg/ml Chl and incubated with 3-(3,4-dichloroprenyl)-1–1-dimethylurea (10 µM DCMU) and hydroxylamine (1 mM HA) to completely block PSII activity. Actinic light was 165 µmol photons m^{-2} s^{-1} for 5 s followed by a flash of saturating light, and then complete darkness. Changes in the redox state of P700 were measured based on optical changes at 705 nm. In panels (*C*) and (*D*), bottom, 1 mM MV was added to the reaction as an electron acceptor for PSI and to inhibit FDX-dependent and NADPH-dependent CEF. Upward arrows present in (*A*), (*C*) and (*D*) represent saturating pulses of light.

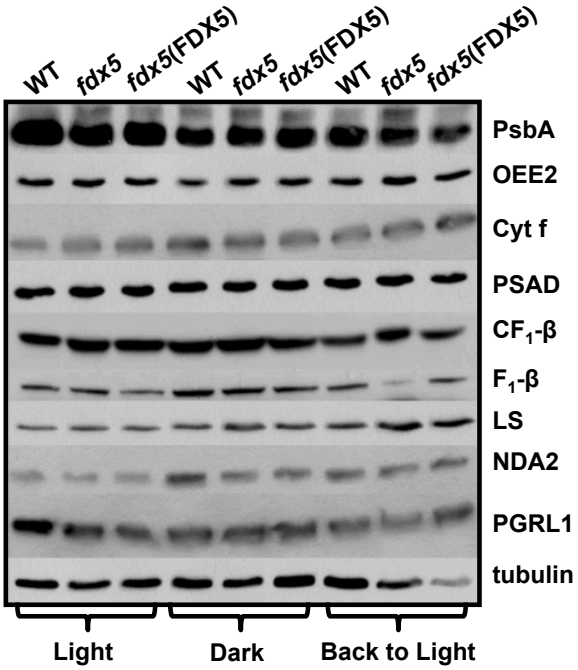

Fig. S8. Immunoblots of representative photosynthetic proteins in different strains. Proteins were resolved by SDS-PAGE (12% polyacrylamide) from 2.5 μg Chl (whole cell) applied per lane. Tubulin was used as a loading control. Samples were collected at 0, 24 h in the dark, and back to light for 24 h (after a 24 h dark period). The proteins examined were PsbA (reaction center protein of PSII), OEE2 (oxygen evolving enhancer complex of PSII), Cyt f (PetA) (subunit of Cyt b_6f complex), PSAD (subunit of PSI), CF1-β (catalytic subunit of chloroplast ATP synthase), F1-β (catalytic subunit of mitochondrial ATP synthase), LS (large subunit of RuBisco), NDA2 (NADPH dehydrogenase protein involved in chlororespiration and NADPH-dependent CEF), PGRL1 (FDX-plastoquinone reductase, which is involved in ferredoxin-dependent CEF), tubulin. The strains used were WT, *fdx5* and *fdx5*(FDX5) rescued strain.

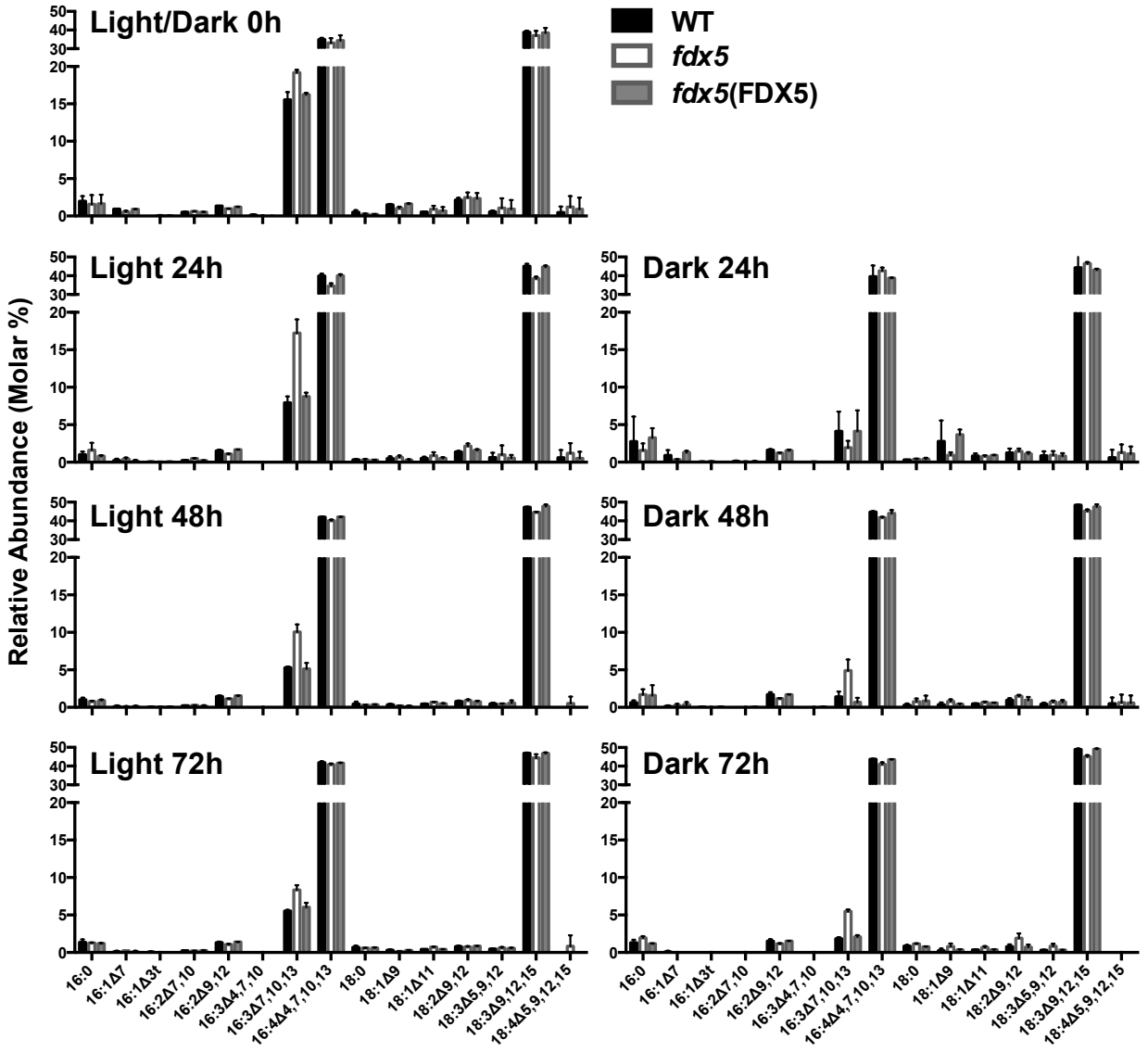

Fig. S9. Profiles of fatty acids in MGDG after growth in the light and dark. Levels of MGDG-associated fatty acids after growth of the cells in the light or dark for 48 and 72 h. Fatty acids are C16 and C18 with the predominant C16 species having 4 double bonds (C16:$4^{\Delta 4,7,10,13}$), while the predominant C18 species has 3 double bonds (C18:$3^{\Delta 9,12,15}$). Error bars, which are barely visible, represent standard deviations. The strains used were WT, *fdx5* and *fdx5*(FDX5) rescued strain.

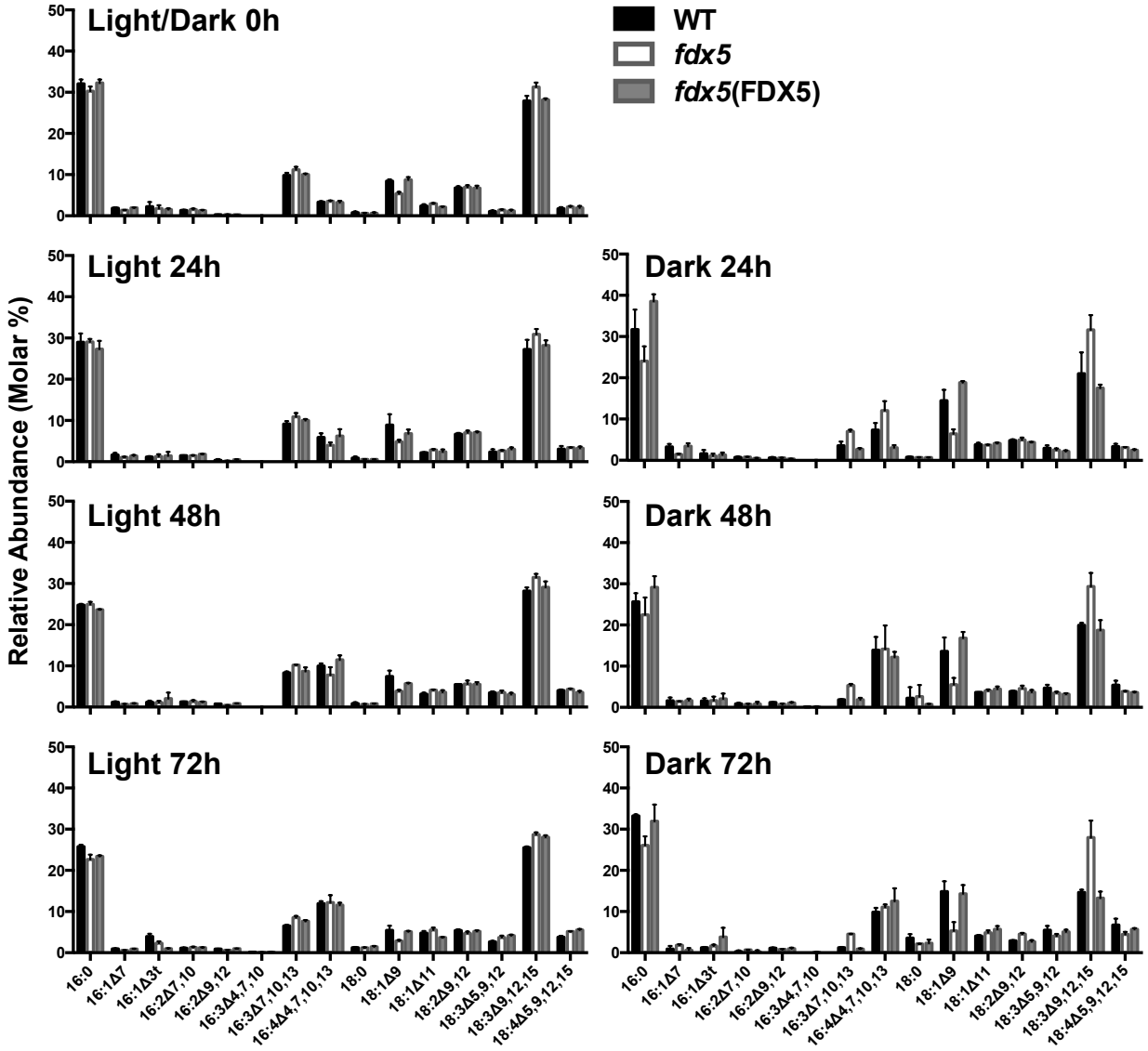

Fig. S10. Profiles of fatty acids in DGDG after growth in the light and dark. Levels of DGDG-associated fatty acids after growth of the cells in the light or dark for 48 and 72 h. Fatty acids are C16 and C18 with the predominant C16 species having 0 (C16:0) and 4 (C16:$4^{\Delta 4,7,10,13}$) double bonds, while the predominant C18 species have 1 (C18:$1^{\Delta 9}$ and C18:$1^{\Delta 11}$), 2 (C18:$2^{\Delta 9,12}$) and 3 (C18:$3^{\Delta 5,\ 9,12,}$ and C18:$3^{\Delta 9,12,15}$) double bonds. Error bars represent standard deviation. The strains used were WT, *fdx5* and *fdx5*(FDX5) rescued strain.

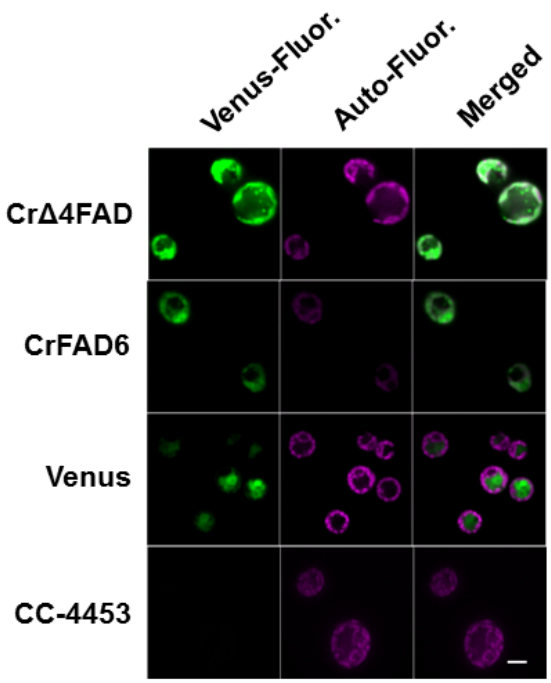

Fig. S11. CrΔ4FAD and CrFAD6 are localized to chloroplasts in Chlamydomonas. The cells either contained the introduced vector with neither *Venus* nor the *FDX5* sequence (CC-4533), with *Venus* (Venus) or with *CrΔ4FAD* or *CrFAD6* fused to Venus (indicated as CrΔ4FAD and CrFAD6). Column 1 shows Venus fluorescence (Venus-Fluor; green fluorescence), column 2 shows Chl auto-fluorescence (Auto-Fluor; magenta fluorescence), column 3 shows the merged image of column 1 and column 2 (green-blue indicates co-localization). The scale bar represents 5 μm.

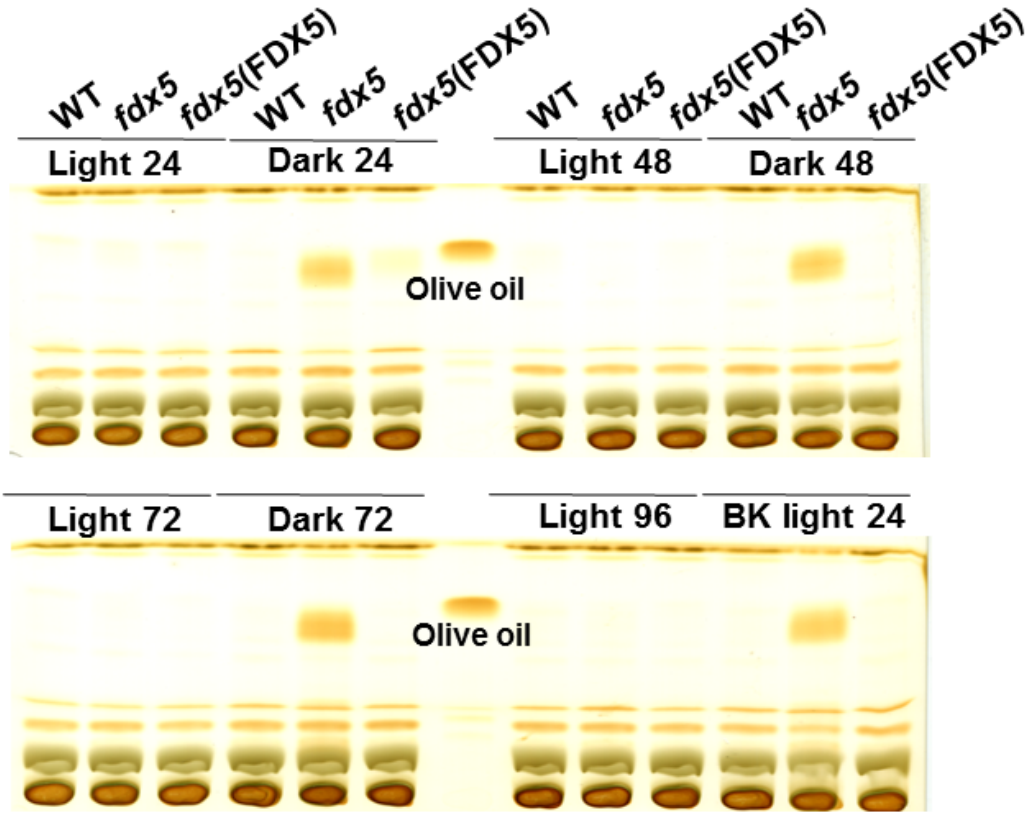

Fig. S12. TAG accumulates in *fdx5* in the dark. Total TAG was separated by thin layer chromatography at 24, 48, 72 h after growth of the cells in the light and dark, and from the dark (72 h) back to light for 24 h (BK light 24). Analyses were performed for WT, the *fdx5* mutant and the *fdx5*(FDX5) complemented strain. 20 μg olive oil was used as the standard.

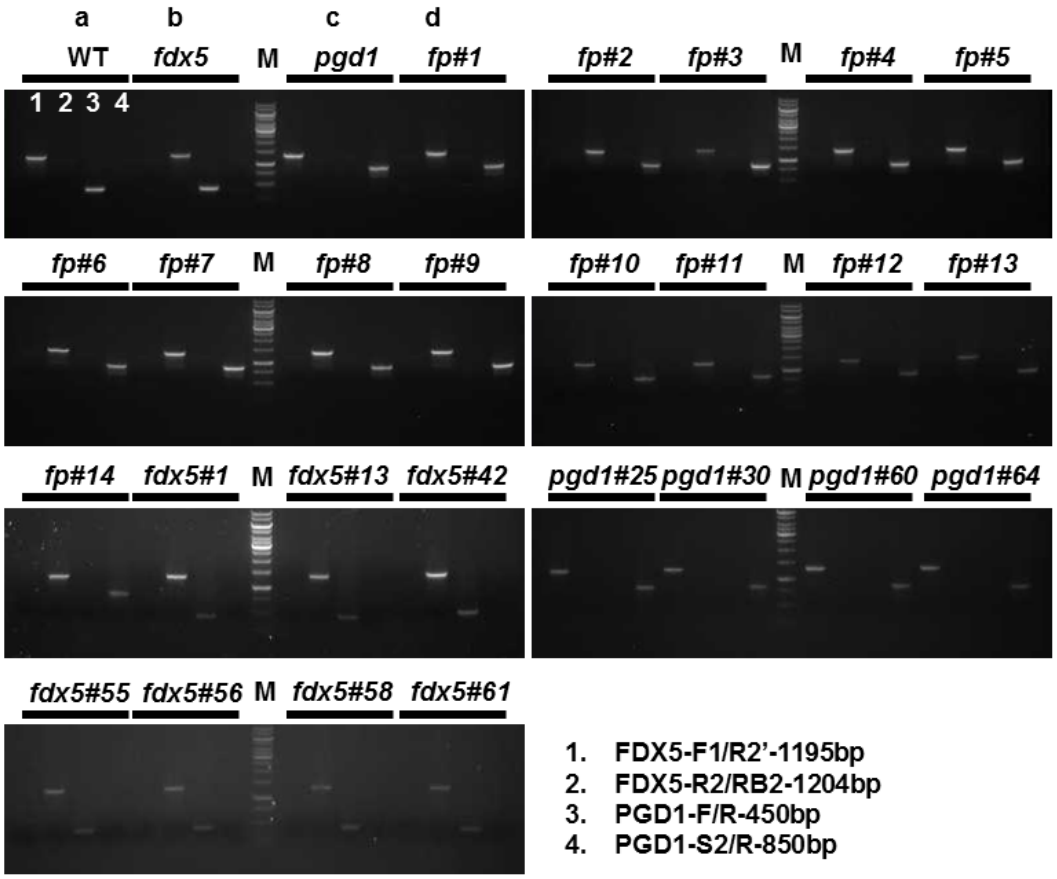

Fig. S13. Genotyping of the *fdx5pgd1* double mutants. *fp* represents the *fdx5pgd1* double mutants. *fdx5* and *pgd1* were used as the parental strains, *fdx5#1*, *fdx5#13*, *fdx5#42*, *fdx5#55*, *fdx5#56*, *fdx5#58*, *fdx5#61* are *fdx5* mutants that segregated in the cross, while the *pgd1#25*, *pgd1#30*, *pgd1#60*, *pgd1#64* were *pgd1* mutants that segregated in the cross. The primers and sizes of the amplification products are listed at the bottom. M represents DNA ladder. The primer pairs (1) FDX5-F1/R2 (for *FDX5*), (2) FDX5-R2/RB2 (for insertion into FDX5), (3) PGD1-F/R (for PGD1), and (4) PGD1-S2/R (for insertion into *PGD1*) were used to genotype the progeny (determine whether or not the strains had an insertion in *FDX5*, *PGD1* or both genes): progeny *a* has intact *FDX5* and *PGD1* genes (WT); progeny *b* has a disrupted *FDX5* and intact *PGD1* gene (*fdx5*); progeny *c* has an intact *FDX5* gene and a disrupted *PGD1* gene (*pgd1*); progeny *d* has a disrupted *FDX5* gene and a disrupted *PGD1* gene (*fdx5pgld1#1*). M represents DNA ladder.

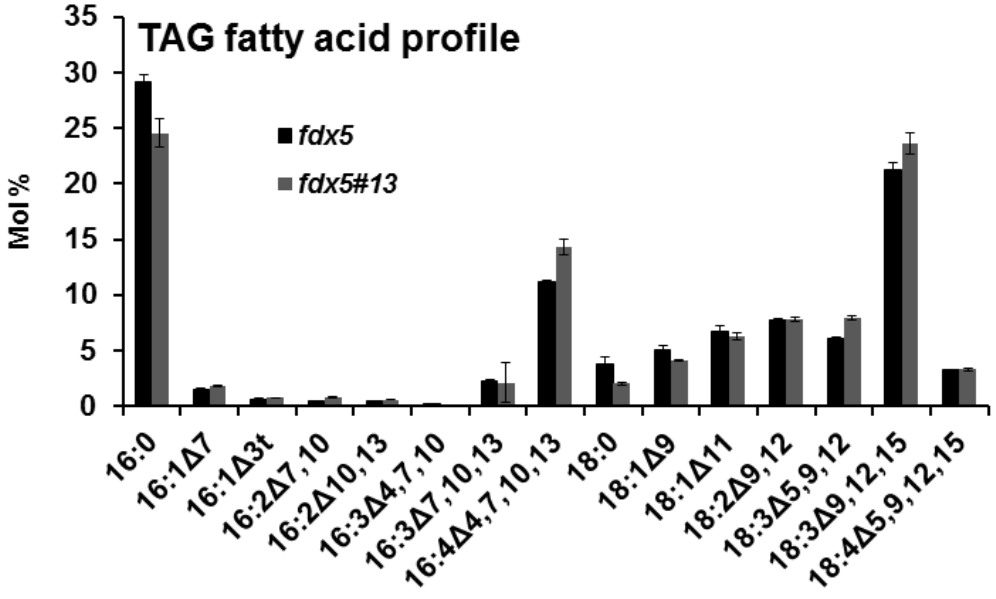

Fig. S14. Fatty acid profiles of *fdx5* and *fdx5*#13 strains that were in the dark for 48 h**.** Error bars represent standard deviation (n=3). The molar percentage of the various fatty acids is given on the y-axis.

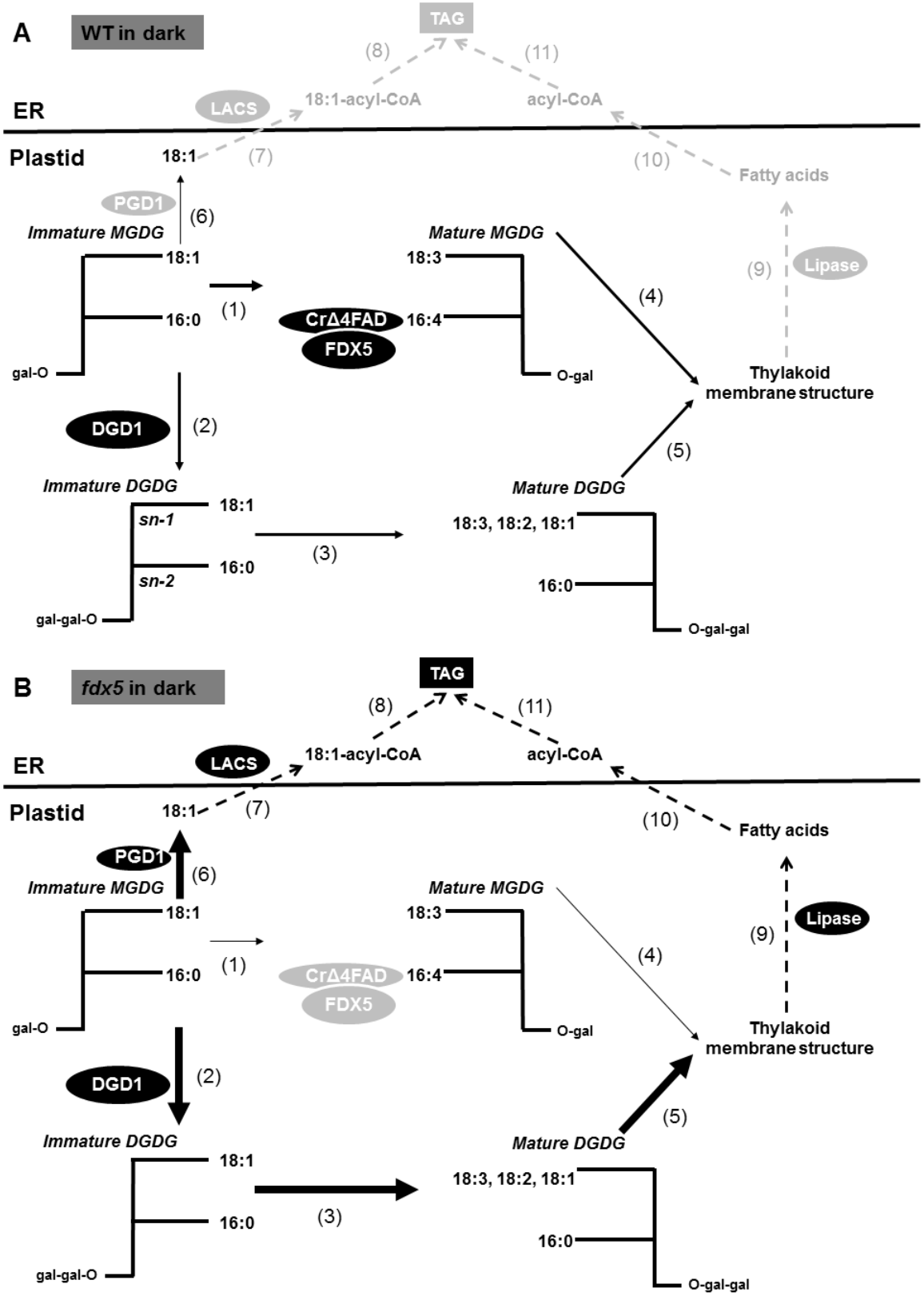
A
WT in dark
TAG
(8)
(11)
ER
LACS
18:1-acyl-CoA
acyl-CoA
Plastid
18:1
(7)
(10)
Fatty acids
PGD1
(6)
Immature MGDG
18:1
16:0
gal-O
(1)
CrΔ4FAD
FDX5
Mature MGDG
18:3
16:4
O-gal
(4)
(9)
Lipase
Thylakoid membrane structure
DGD1
(2)
Immature DGDG
sn-1
18:1
sn-2
16:0
gal-gal-O
(3)
Mature DGDG
(5)
18:3, 18:2, 18:1
16:0
O-gal-gal
B
fdx5 in dark
TAG
(8)
(11)
ER
LACS
18:1-acyl-CoA
acyl-CoA
Plastid
18:1
(7)
(10)
Fatty acids
PGD1
(6)
Immature MGDG
18:1
16:0
gal-O
(1)
CrΔ4FAD
FDX5
Mature MGDG
18:3
16:4
O-gal
(4)
(9)
Lipase
Thylakoid membrane structure
DGD1
(2)
Immature DGDG
18:1
16:0
gal-gal-O
(3)
Mature DGDG
(5)
18:3, 18:2, 18:1
16:0
O-gal-gal

Fig. S15. Model for FDX5-mediated regulation of thylakoid membrane structure in the dark. The filled shapes and arrows represent proteins/enzymes and reactions, respectively. The black and grey colors represent the active and inactive status of the enzymes or reactions, respectively; and the thickness of the arrows represents the extent of the biosynthetic reactions. (*A*) Model for WT cells. (*B*) Model for the *fdx5* mutant. In the dark, the immature MGDG can be converted to a number of different products: (1) conversion of immature to mature MGDG by desaturation of C18:1 at *sn-1* and C16:0 at *sn-2* to C18:3 and C16:4 through CrFAD6 and CrΔ4FAD, respectively, with electron donation potentially from FDX5; (2) conversion from immature MGDG to immature DGDG through addition of a second galactose head group to the MGDG, which is catalyzed by DGD1 (digalactosyldiacylgycerol synthase); (3) conversion of immature DGDG to mature DGDG by desaturation of the C18:1 at *sn-1* position to C18:3 through the activity of CrFAD6 and electron donation potentially from FDX5; (4 and 5) integration of mature MGDG and DGDG into thylakoid membranes; (6) conversion of immature MGDG to lyso-immature MGDG by PGD1-dependent cleaving of C18:1 from the *sn-1* position; (7) conversion of cleaved C18:1 from plastid MGDG to C18:1-acyl-CoA by LACS (long chain acyl-CoA synthetase) in the ER; (8) recruitment of C18:1-acyl-CoA for TAG synthesis; (9) degradation of thylakoid membrane by lipases to release free fatty acids in plastid; (10) movement of free fatty acids from plastid to ER to generate acyl-CoA; (11) recruitment of the free acyl-CoA for TAG synthesis in the ER. The inability to perform (1) would promote (2) and (6). Fatty acids in addition to C18 can also be recruited for TAG formation.

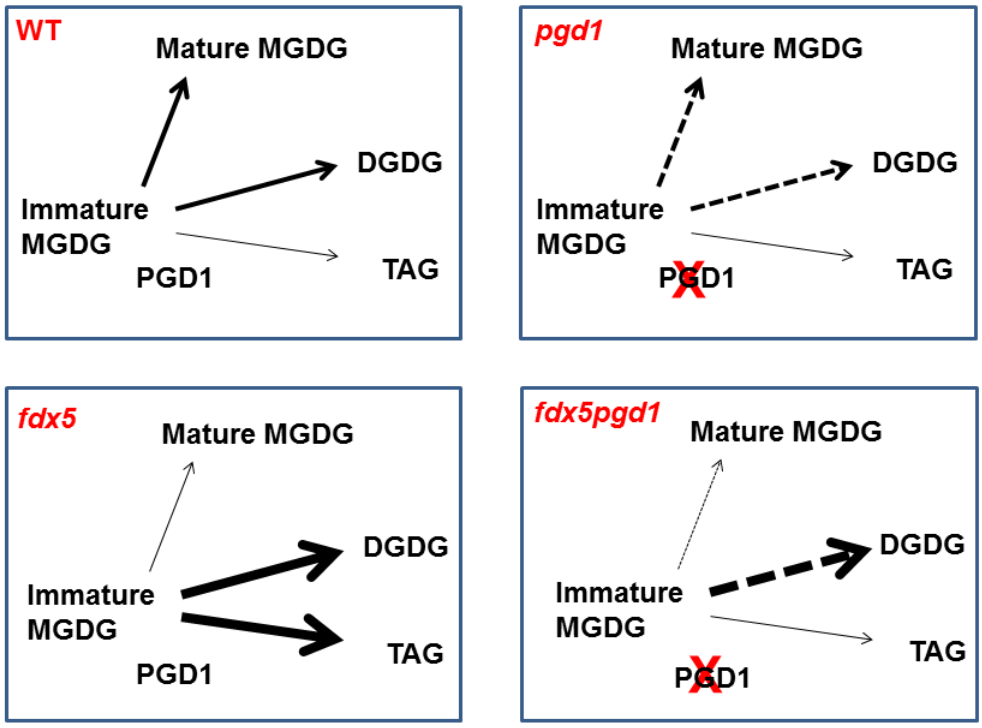

Fig. S16. The impact of PGD1 on lipid production in the various strains in the dark. The arrows are of different thicknesses, indicating a relative level of immature MGDG that is converted to various products. The dashed lines represent possible metabolic fates in the *pgd1* mutant.

Tables S1-S5

Table S1. Genes encoding ferredoxins in the Chlamydomonas genome.

PredAlgo software (https://giavap-genomes.ibpc.fr/cgi-bin/predalgodb.perl?page=main)[26] was used to predict the subcellular localization of Ferredoxins. Names, protein IDs, NCBI accession numbers, and predicted localizations are indicated.

Gene	JGI v4.0	Phytozome v10.0.4	NCBI	Localization
FDX1(Fd)	147787	g15094	XP_001692808.1	Chloroplast
FDX2	159161	Cre16.g658400	XP_001697912.1	Chloroplast
FDX3	196707	Cre06.g306350	XP_001691381.1	Chloroplast
FDX4	196705	Cre07.g334800	XP_001700106.1	Chloroplast
FDX5	156833	Cre17.g700950	XP_001691603.1	Chloroplast
FDX6	196703	Cre03.g183850	XP_001702961.1	Chloroplast
FDX7	160049	Cre01.g006100	XP_001702098.1	Chloroplast
FDX8	179658	Cre01.g005600	XP_001702123.1	Chloroplast
FDX9	188740	Cre12.g487900	XP_001690910.1	Chloroplast
FDX10	189455	Cre04.g225450	XP_001692319.1	Chloroplast
FDX11	174881	Cre06.g291650	XP_001695531.1	Chloroplast
FDX12	205989	Cre08.g374550	-	?
MFDX	154720	Cre12.g559950	XP_001703155.1	Mitochondria

Table S2. Primers used in this study

Primer names	Use of primers	Orientation	Sequence	Tm
FDX5-F1	Mutant screen	forward	5'- GCATTGCCTAACAGCCTTACCTCCA -3'	60.0°C
FDX5-R1	Mutant screen	reverse	5'- CCCAACAACCGTGTGTGCCACGCTTC -3'	60.0°C
FDX5-F2	Mutant screen	forward	5'- GAAGCGTGGCACACACGGTTGTTGGG -3'	60.0°C
FDX5-R2	Mutant screen	reverse	5'- TACTGGTGCTTGCCGTACTC -3'	60.0°C
FDX5-F3	Mutant screen	forward	5'- GAGTACGGCAAGCACCAGTA -3'	60.0°C
FDX5-R3	Mutant screen	reverse	5'- ATCAGTCCCATCCTCAACCAATCCTCA CG -3'	60.0°C
FDX5-COM-F	Complementation	forward	5'- GAATTCATTACACAGCAGTTTCAGGCAT T -3'	59.7°C
FDX5-COM-R	Complementation	reverse	5'- TAGGATCCCCATAGTTGGGGGTTACATG AA-3'	58.8°C
RB1	Insert localization	forward	5'- ATGGGGCGGTATCGGAGGAAAAG -3'	60.0°C
RB2	Insert localization	forward	5'- TACCGGCTGTTGGACGAGTTCTTCTG -3'	60.0°C
RIM1	Insert localization	reverse	5'- GCTGGCACGAGTACGGGTTG -3'	58.0°C
Mid-up	Mating type	forward	5'- ATGGCCTGTTTCTTAGC -3'	52.0°C
Mid-low	Mating type	reverse	5'- CTACATGTGTTTCTTGACG -3'	52.0°C
Fus-up	Mating type	forward	5'- ATGCCTATCTTTCTCATTCT -3'	52.0°C
Fus-low	Mating type	reverse	5'- GCAAAATACACGTCTGGAAG -3'	52.0°C
FDX5Loc	Localization	forward	5'-GGTTAACATGCTGTGCGCGCGCTCCC-3'	60.0°C
FDX5Loc	Localization	reverse	5'-GGTTAACCTGGTGCTTGCCGTACTCG-3'	60.0°C
APH8-F1	Southern blot probe	forward	5'-ATGGACGATGCGTTGCGT-3'	66.0°C
APH8-R1	Southern blot probe	reverse	5'-CTCAGAAGAACTCGTCCAACA-3'	62.0°C
FDX5-F4	Southern blot probe	forward	5'-TACTCCCTTCCGACCCACATCCTGA-3'	72.0°C
FDX5-R4	Southern blot probe	reverse	5'-GACCCCACCTTACCCCACATCAG-3'	70.0°C
PGD1-F	Genotyping	forward	5'- ACATCGTGAATGGCAAAACA -3'	60.0°C
PGD1-R	Genotyping	reverse	5'- ATTGCGCGGGTTTAGAACTT -3'	60.0°C
PGD1-S2-1	Genotyping	forward	5'- ATAGGGGTTCCGCGCACAT -3'	70.0°C
FDX5-Y2H-F	Y2H	forward	5'- CACCATGCTGTGCGCGCGCTCCCAGC -3'	60.0°C
FDX5-Y2H-R	Y2H	reverse	5'- TTACTGGTGCTTGCCGTACT -3'	60.0°C
FD-Y2H-F	Y2H	forward	5'- CACCATGGCCATGGCTATGCGCTC -3'	60.0°C
FD-Y2H-R	Y2H	reverse	5'- GTACAGGGCCTCCTCCTGGTG -3'	60.0°C
CrΔ4FAD-Y2H-F	Y2H	forward	5'- CACCATGAACGCCACGATGCAGCG -3'	60.0°C
CrΔ4FAD-Y2H-R	Y2H	reverse	5'- TTAGAACTTGGAGAGCATCAGCATCTCG C -3'	60.0°C
CrFAD6-Y2H-F	Y2H	forward	5'- CACCATGGCGTTCGCTCTGCGCTC -3'	60.0°C
CrFAD6-Y2H-R	Y2H	reverse	5'- TTAGAAGGCGGCGGAGTCGG -3'	60.0°C
FDX5_Venus –F	Gibson Cloning	forward	5'- GCTACTCACAACAAGCCCAGTTATGCTG TGCGCGCGCTCCCAGC -3'	60.0°C
FDX5_Venus –R	Gibson Cloning	reverse	5'- GAGCCACCCAGATCTCCGTTCTGGTGCTT GCCGTACT -3'	60.0°C
CrΔ4FAD_Venus –F	Gibson Cloning	forward	5'-GCTACTCACAACAAGCCCAGTTATGAAC GCCACGATGCAGCG -3'	60.0°C
CrΔ4FAD_Venus –R	Gibson Cloning	reverse	5'- GAGCCACCCAGATCTCCGTTGAACTTGG AGAGCATCAGCATCTCGC -3'	60.0°C

CrFAD6_Venus –F	Gibson Cloning	forward	5'- GCTACTCACAACAAGCCCAGTTATGGCG TTCGCTCTGCGCTC -3'	60.0°C
CrFAD6_Venus –R	Gibson Cloning	reverse	5'- GAGCCACCCAGATCTCCGTTGAAGGCGG CGGAGTCGG -3'	60.0°C
oMJ237	Gibson sequencing	forward	5’- GGAGGTACGACCGAGATGGCT-3’	60.0°C
oMJ555	Venus sequencing	reverse	5’-CACGTCGCCGTCCAGCTC -3’	60.0°C
oMJ556	mCherry sequencing	reverse	5’- CTCCTTGATGATGGCCATG-3’	60.0°C

Table S3. Strains used in this study

Name	Note	Background
CC124/5	Wild-type - mating type pair	*nit1nit2*
D66	Wild-type - CC-4425	*nit2, cw15, mt*$^{+}$
21gr(+/-)	Wild-type - mating type pair	*NIT1, NIT2*
cMJ030	Wild-type - from 4A x D66 cross, CC-4533	*nit1nit2cw15*
fdx5 in D66	The mutant was generated in D66	*nit1nit2cw15, Paro*$^{+}$
fdx5 in CC124/5	Backcross of *fdx5* into CC124/5	*nit1nit2, Paro*$^{+}$
fdx5 in 21gr	Backcross of *fdx5* into 21gr(+/-)	*NIT1, NIT2, Paro*$^{+}$
dw15	CC-4619	*nit1nit2cw15*
pgd1 in dw15	CC-4593	*nit1nit2cw15, Hyg*$^{+}$
fdx5#	Segregated from cross of *fdx5pgd1*	*nit1nit2, Paro*$^{+}$
pgd1#	Segregated from cross of *fdx5pgd1*	*nit1nit2, Hyg*$^{+}$
fdx5pgd1	Segregated from cross of *fdx5pgd1*	*nit1nit2, Paro*$^{+}$*, Hyg*$^{+}$
pLM005FDX5	Transformed to cMJ030, for localization	*nit1nit2, Paro*$^{+}$
pLM005CrΔ4FAD	Transformed to cMJ030, for localization	*nit1nit2, Paro*$^{+}$
pLM005CrFAD6	Transformed to cMJ030, for localization	*nit1nit2, Paro*$^{+}$
fdx5(FDX5) -1	By *FDX5*-cDNA	*nit1nit2, Paro*$^{+}$*, Zeo*$^{+}$
fdx5(FDX5) -2	By *FDX5*-gDNA	*nit1nit2, Paro*$^{+}$*, Zeo*$^{+}$

Table S4. Constructs used in this study

Use	Construct	Plasmid name	Insert or PCR product	Primers	Plasmid backbone	Cloning method
Localization	Venus	pLM005_Venus	-	-	pUC19	-
	Venus:FDX5	pLM005FDX5_Venus	FDX5 CDS	FDX5_Venus –F/ FDX5_Venus –R	pUC19	Gibson Cloning
	Venus:CrΔ4FAD	pLM005 CrΔ4FAD _Venus	CrΔ4FAD CDS	CrΔ4FAD_Venus –F/ CrΔ4FAD_Venus –R	pUC19	Gibson Cloning
	Venus:CrFAD6	pLM005 CrFAD6 _Venus	CrFAD6 CDS	CrFAD6_Venus –F/ CrFAD6_Venus –R	pUC19	Gibson Cloning
Mating-based split ubiquitin system (mbSUS)	D-TOPO:FD	pENTR/D-TOPO_FD	FD CDS	FD-Y2H –F/ FD-Y2H –R	pENTR	D-TOPO Cloning
	D-TOPO:FDX5	pENTR/D-TOPO_FDX5	FDX5 CDS	FDX5-Y2H –F/ FDX5-Y2H –R	pENTR	D-TOPO Cloning
	D-TOPO: CrΔ4FAD	pENTR/D-TOPO_ CrΔ4FAD	CrΔ4FAD CDS	CrΔ4FAD-Y2H-F/ CrΔ4FAD-Y2H-R	pENTR	D-TOPO Cloning
	D-TOPO: CrFAD6	pENTR/D-TOPO_ CrFAD6	CrFAD6 CDS	CrFAD6-Y2H-F/ CrFAD6-Y2H-R	pENTR	D-TOPO Cloning
	NubG	pXN22	-	-	pUC	-
	FD:NubG	pXN22_FDX1	FD CDS	FD-Y2H –F/ FD-Y2H –R	pUC	LR Cloning
	FDX5:NubG	pXN22_FDX5	FDX5 CDS	FDX5-Y2H –F/ FDX5-Y2H –R	pUC	LR Cloning
	Cub	pMet-YC	-	-	pUC	-
	Cub:CrΔ4FAD	pMet-YC_CrΔ4FAD	CrΔ4FAD CDS	CrΔ4FAD-Y2H-F/ CrΔ4FAD-Y2H-R	pUC	LR Cloning
	Cub:CrFAD6	pMet-YC_CrΔ4FAD	CrFAD6 CDS	CrFAD6-Y2H-F/ CrFAD6-Y2H-R	pUC	LR Cloning
Complementation	PSAD:FDX5 cDNA	pJM43Ble_FDX cDNA	FDX5 cDNA	FDX5-COM-F1/ FDX5-COM-R1	pSP124	EcoRI/BamHI
	PSAD:FDX5 gDNA	pJM43Ble_FDX gDNA	FDX5 gDNA	FDX5-COM-F1/ FDX5-COM-R1	pSP124	EcoRI/BamHI

Table S5. Pull down assay using FDX5 to establish interacting proteins

Name	ID Number	Annotation	Accession ID	MW[1]	Hits[2]
FDX5	Cre17.g700950	apoferredoxin	gi|159466834	14 kDa	8
chlorophyll a/b binding protein					
LHCBM6	Cre06.g285250	chlorophyll a/b binding protein of LHCII	gi|159474480	27 kDa	7
LHCA5	Cre10.g425900	chlorophyll a/b binding protein of LHCI	gi|159489490	28 kDa	6
LHCBM1	Cre01.g066917	chlorophyll a/b binding protein of LHCII	gi|20269804	28 kDa	4
LHCB5	Cre16.g673650	chlorophyll a/b binding protein of LHCII	gi|159475641	31 kDa	4
LHCBM2	Cre12.g548400	chlorophyll l a/b binding protein of LHCII	gi|159471686	27 kDa	4
LHCB4	Cre17.g720250	chlorophyll a/b binding protein of LHCII	gi|159478202	30 kDa	4
LHCA7	Cre16.g687900	chlorophyll a/b binding protein of LHCI	gi|40714521	26 kDa	4
LHCA4	Cre10.g452050	chlorophyll a/b binding protein of LHCI	gi|40714509	29 kDa	4
LHCA3	Cre11.g467573	chlorophyll a/b binding protein of LHCI	gi|40714511	29 kDa	4
LHCA9	Cre07.g344950	chlorophyll a/b binding protein of LHCI	gi|159468772	23 kDa	3
LHCA8	Cre06.g272650	chlorophyll a/b binding protein of LHCI	gi|159476206	26 kDa	3
LHCBM5	Cre03.g156900	chlorophyll a/b binding protein of LHCII	gi|159478875	29 kDa	3
LHCA6	Cre06.g278213	chlorophyll a/b binding protein of LHCI	gi|159479992	28 kDa	3
LHCA2	Cre12.g508750	chlorophyll a/b binding protein of LHCI	gi|159465641	27 kDa	3
LHCBM3	Cre04.g232104	chlorophyll a/b binding protein of LHCII	gi|159491492	27 kDa	2
Ribosomal protein					
PRL4	Cre09.g397697	ribosomal protein L4	gi|159473354	45 kDa	8
PRL6	Cre01.g011000	ribosomal protein L6	gi|159463286	24 kDa	7
PRPL7	Cre13.g581650	plastid ribosomal protein L7/L12	gi|159470865	14 kDa	6
RPS7	Cre12.g498900	ribosomal protein S7	gi|159488703	22 kDa	6
RPL13	Cre14.g630100	ribosomal protein L13	gi|159469029	24 kDa	5
RPS3	Cre11.g467702	ribosomal protein S3	gi|213517427	82 kDa	5
RPL18A	Cre01.g047750	ribosomal protein L18a	gi|159463026	21 kDa	5
RPS3	Cre02.g102250	ribosomal protein S3	gi|159483497	26 kDa	4
PRPL4	Cre11.g479500	plastid ribosomal protein L4	gi|159478579	26 kDa	4
RPP0	Cre12.g520500	acidic ribosomal protein P0	gi|159477927	35 kDa	4
RPL7A	Cre12.g529651	ribosomal protein L7a	gi|159477735	29 kDa	4
PRPL1	Cre02.g088900	plastid ribosomal protein L1	gi|159487501	32 kDa	4
RPL21	Cre06.g278135	ribosomal protein L21	gi|159479900	18 kDa	4
PRPL31	Cre48.g761197	plastid ribosomal protein L3	gi|159485314	28 kDa	4
RPS13	Cre07.g331900	ribosomal protein S13	gi|159464389	17 kDa	4
PSRP3	Cre02.g083950	plastid-specific ribosomal protein 3	gi|159487801	33 kDa	4
PRPL9	Cre12.g556050	plastid ribosomal protein L9	gi|159472060	22 kDa	3
RPL19	Cre02.g075700	ribosomal protein L19	gi|159487227	23 kDa	3
RPS3a	Cre13.g568650	ribosomal protein S3a	gi|159471131	29 kDa	3
RPL10	Cre09.g388200	ribosomal protein L10	gi|159472591	26 kDa	3
RPL14	Cre17.g701200	ribosomal protein L14	gi|159466828	15 kDa	3
RPL11	Cre01.g027000	ribosomal protein L11	gi|159463566	20 kDa	3

RPL12	Cre12.g528750	ribosomal protein L12	gi|159477751	18 kDa	3
RPS5	Cre06.g290950	ribosomal protein S5	gi|159474574	22 kDa	3
RPL11	Cre01.g027000	ribosomal protein L5	gi|126165895	20 kDa	3
RPS14	Cre11.g480150	ribosomal protein S14	gi|159478595	16 kDa	3
PRPS5	Cre16.g659950	plastid ribosomal protein S5	gi|159479560	72 kDa	3
RPS24	Cre10.g456200	ribosomal protein S24	gi|159480596	15 kDa	3
RPS16	Cre13.g573351	ribosomal protein S16	gi|159470701	16 kDa	3
RPS4	Cre06.g308250	ribosomal protein S4	gi|159466042	29 kDa	3
RPS6	Cre09.g400650	ribosomal protein S6	gi|159473970	28 kDa	2
RPS28	Cre12.g510450	ribosomal protein S28	gi|159465687	7 kDa	2
RPS8	Cre06.g272800	ribosomal protein S8	gi|159476204	24 kDa	2
RPL13A	Cre12.g532550	ribosomal protein L13a	gi|159469516	21 kDa	2
PRPL6	Cre09.g415950	plastid ribosomal protein L6	gi|159477461	22 kDa	2
PRPL31	Cre08.g365400	plastid ribosomal protein L31	gi|159476036	15 kDa	2
RPL9	Cre12.g494050	ribosomal protein L9	gi|159484990	22 kDa	2
RPL7	Cre12.g537800	ribosomal protein L7	gi|159469644	30 kDa	2
RPS15	Cre08.g360900	ribosomal protein S15	gi|159475964	17 kDa	2
PRPL19	Cre17.g734450	plastid ribosomal protein L19	gi|159469822	17 kDa	2
Translation factor					
EEF1A3	Cre06.g263450	eukaryotic translation elongation factor 1 alpha 1	gi|159476938	51 kDa	17
EFG8	Cre06.g259150	elongation factor Tu	gi|41179007	46 kDa	6
EIF3G	Cre06.g269450	eukaryotic translation initiation factor	gi|159476822	31 kDa	3
EFG2	Cre12.g516200	elongation factor 2	gi|159490505	94 kDa	2
HEL30	Cre06.g298650	eukaryotic initiation factor 4A-like protein	gi|159466510	47 kDa	4
Cytoskeleton					
TUB1	Cre12.g542250	beta tubulin 2	gi|159471706	50 kDa	11
TUA2	Cre04.g216850	alpha tubulin 1	gi|159467393	50 kDa	9
ACT1	Cre13.g603700	actin	gi|159482014	42 kDa	3
ATP synthase					
mATP2	Cre17.g698000	ATP synthase subunit beta, chloroplastic	gi|226698718	52 kDa	9
ATP2	Cre17.g698000	beta subunit of mitochondrial ATP synthase	gi|159466892	62 kDa	9
ATP1A	Cre02.g116750	ATP synthase CF1 alpha subunit	gi|213517431	55 kDa	7
ATPG	Cre11.g481450	CF0 ATP synthase subunit II precursor	gi|159478483	22 kDa	2
ASA1	Cre07.g340350	mitochondrial F1F0 ATP synthase associated protein	gi|159468466	63 kDa	3
ATP1A	Cre02.g116750	mitochondrial F1F0 ATP synthase, alpha subunit	gi|159483185	62 kDa	2
ASA2	Cre09.g415550	mitochondrial F1F0 ATP synthase associated protein	gi|159477287	48 kDa	4
Photosynthesis related protein					
PSBP1	Cre12.g550850	Oxygen-evolving enhancer protein 2	gi|131389	26 kDa	9
PsbB	Cre09.g416200	photosystem II 47 kDa protein	gi|213517415	56 kDa	8
PSBQ	Cre08.g372450	oxygen evolving enhancer protein 3	gi|159486609	22 kDa	8
PSBO	Cre09.g396213	oxygen-evolving enhancer protein 1	gi|159473144	31 kDa	8
PsbC	Cre09.g388356	photosystem II 44 kDa protein	gi|41179065	51 kDa	5
PSAF	Cre09.g412100	photosystem I reaction center subunit III	gi|159477399	24 kDa	4

PsaB	Cre17.g702500	photosystem I subunit PsaB	gi|41179048	82 kDa	3
PETO	Cre12.g558900	cytochrome b6f complex subunit V	gi|159489663	20 kDa	2
D2	Cre07.g317201	photosystem II protein D2	gi|225115	41 kDa	3
PSAD	Cre05.g238332	photosystem I reaction center subunit II	gi|159479282	21 kDa	2
CGLD37	Cre09.g392350	glycine-rich RNA-binding protein	gi|159472653	16 kDa	5
CPLD20	Cre01.g000900	predicted protein	gi|159484580	46 kDa	3
ASC1	Cre01.g013700	predicted protein	gi|159462440	28 kDa	2
RCA1	Cre04.g229300	rubisco activase	gi|159468147	45 kDa	4
PHT1	Cre03.g199000	phototropin	gi|159470479	81 kDa	2
Lipid metabolism					
FAB2	Cre17.g701700	plastid acyl-ACP desaturase	gi|159466822	45 kDa	7
ACX2	Cre12.g519100	acetyl-CoA carboxylase	gi|159477697	54 kDa	3
Chaperon					
HSP70A	Cre08.g372100	heat shock protein 70A	gi|159486599	71 kDa	2
HSP70B	Cre06.g250100	heat shock protein 70B	gi|1225970	72 kDa	6
CPN60B2	Cre07.g339150	chaperonin 60B2	gi|159468684	62 kDa	2
RUBA	Cre04.g231222	chaperonin 60A	gi|159491478	62 kDa	4
Nucleotide metabolism					
PNBP	Cre06.g269050	pyridine nucleotide binding protein	gi|159476278	75 kDa	4
ANT1	Cre09.g386650	adenine nucleotide translocator	gi|159474120	34 kDa	4
AAA1	Cre08.g358526	plastidic ADP/ATP translocase	gi|159491564	62 kDa	3
Starch metabolism					
AGP1	Cre13.g567950	ADP-glucose pyrophosphorylase large subunit	gi|159470605	55 kDa	4
GAD1	Cre03.g169400	UDP-D-glucuronic acid decarboxylase	gi|159491066	37 kDa	3
SBP1	Cre03.g185550	sedoheptulose-1,7-bisphosphatase	gi|159467635	42 kDa	3
PRK1	Cre12.g554800	phosphoribulokinase	gi|159471788	42 kDa	3
Anoxia					
PFL1	Cre01.g044800	pyruvate-formate lyase	gi|159462978	91 kDa	4
ADH1	Cre17.g746997	aldehyde-alcohol dehydrogenase	gi|92084840	102 kDa	4
ATO1	Cre17.g723650	acetyl-CoA acyltransferase	gi|159478266	47 kDa	3
FUM1	Cre06.g254400	fumarate hydratase	gi|159477070	63 kDa	5
GAP1	Cre12.g485150	Glyceraldehyde-3-phosphate dehydrogenase	gi|1346064	37 kDa	3
ALS2	Cre01.g055453	acetolactate synthase	gi|159484278	52 kDa	3
Histone					
HFO11	Cre06.g266600	histone H4	gi|159464880	11 kDa	3
HTA17	Cre12.g505550	histone H2A	gi|159464886	14 kDa	2
Mitochondria metabolism					
QCR2	Cre12.g509750	mitochondrial processing peptidase alpha subunit	gi|159465665	50 kDa	3
COX90	Cre16.g691850	cytochrome c oxidase subunit	gi|159482474	12 kDa	2
QCR7	Cre06.g262700	ubiquinol:cytochrome c oxidoreductase 14 kDa subunit	gi|159476418	14 kDa	2
Various metabolism					
GAP3	Cre01.g010900	glyceraldehyde-3-phosphate dehydrogenase	gi|159463282	40 kDa	5
CIS2	Cre03.g149100	citrate synthase	gi|159474920	55 kDa	5

AST1	Cre09.g387726	aspartate aminotransferase	gi|159473837	47 kDa	6
MES1	Cre03.g180750	cobalamin-independent methionine synthase	gi|159489910	87 kDa	12
PRX2	Cre02.g114600	2-cys peroxiredoxin	gi|159483223	22 kDa	4
APR1	Cre12.g517150	adenylylphosphosulfate reductase	gi|159477975	46 kDa	3
IDH2	Cre02.g143250	NAD-dependent isocitrate dehydrogenase	gi|159473471	39 kDa	2
MAS1	Cre03.g144807	malate synthase	gi|159475042	61 kDa	2
ACH1	Cre01.g042750	aconitate hydratase	gi|159462944	86 kDa	2
MAP	Cre06.g254917	minus agglutinin protein	gi|159477066	255 kDa	2
SHMT1	Cre16.g664550	serine hydroxymethyltransferase	gi|159486853	57 kDa	2
Signal transduction					
TEF2	Cre12.g497300	calcium sensing receptor	gi|46093489	39 kDa	5
NOP58	Cre10.g441400	nucleolar protein, component of C/D snoRNPs	gi|159464245	55 kDa	2
MAPK6	Cre12.g508900	mitogen-activated protein kinase 6	gi|159465279	43 kDa	2
CDPK1	Cre17.g705000	calcium-dependent protein kinase 1	gi|159466768	67 kDa	2
CAV8	Cre12.g532350	voltage-gated Ca2+ channel, alpha subunit	gi|159469522	471 kDa	2
Unknown protein					
Unknown	Cre03.g145507	hypothetical protein	gi|159475228	28 kDa	5
FAP24	Cre02.g081050	flagellar associated protein	gi|159487357	57 kDa	5
Unknown	no ID	Chain A, N153q Mutant Of Cytochrome F	gi|10121062	27 kDa	4
HEL47	Cre10.g427700	predicted protein	gi|159489124	63 kDa	3
TEF10a	Cre03.g146167	hypothetical protein	gi|159474984	25 kDa	3
Unknown	Cre02.g112150	hypothetical protein	gi|159483731	35 kDa	3
Unknown	Cre03.g197450	predicted protein	gi|159469995	132 kDa	2
Unknown	Cre06.g263250	predicted protein	gi|159476406	65 kDa	2

Note: [1] represents protein molecular weight; [2] represents the numbers of hits from the pull-down assay.

Supplemental References

1. Xie Z, Merchant S (1996) The plastid-encoded *ccsA* gene is required for heme attachment to chloroplast c-type cytochromes. *J Biol Chem* 271(9):4632-4639.
2. Yang W*, et al.* (2014) Alternative acetate production pathways in *Chlamydomonas reinhardtii* during dark anoxia and the dominant role of chloroplasts in fermentative acetate production. *Plant Cell* 26(11):4499-4518.
3. Gibson DG*, et al.* (2009) Enzymatic assembly of DNA molecules up to several hundred kilobases. *Nat Methods* 6(5):343-345.
4. Rasala BA*, et al.* (2013) Expanding the spectral palette of fluorescent proteins for the green microalga *Chlamydomonas reinhardtii*. *Plant J* 74(4):545-556.
5. Takahashi H, Iwai M, Takahashi Y, Minagawa J (2006) Identification of the mobile light-harvesting complex II polypeptides for state transitions in *Chlamydomonas reinhardtii*. *Proc Natl Acad Sci U S A* 103(2):477-482.
6. Radmer RJ, Kok B (1976) Photoreduction of O_2 primes and replaces CO_2 assimilation. *Plant Physiol* 58(3):336-340.
7. Heinnickel ML*, et al.* (2013) Novel thylakoid membrane GreenCut protein CPLD38 impacts accumulation of the cytochrome b6f complex and associated regulatory processes. *J Biol Chem* 288(10):7024-7036.
8. Peden EA*, et al.* (2013) Identification of global ferredoxin interaction networks in *Chlamydomonas reinhardtii*. *J Biol Chem* 288(49): 35192-35209.
9. Merchant SS*, et al.* (2007) The *Chlamydomonas* genome reveals the evolution of key animal and plant functions. *Science* 318(5848):245-250.

Genomic DNA sequence of the *fdx5* mutant. The blue uppercase letters represent UTR regions, the red uppercase letters represent exons, and the black uppercase letters represents intron. The lowercase letters represent the insertion cassette.

ATTACACAGCAGTTTCAGGCATTGCCTAACAGCCTTACCTCCAAACCCTTGCCCCGACCTGTCCGTCGC
GACTCTTCCGAAAGAATGCTGTGCGCGCGCTCCCAGCTGGTCTGCAAGCCTGTGAAGGCTGCTCGCGC
CTCTCGCGCTACCGTCAAGGTGCGCACCGACCGGTATCGCGTTCAGGTTGAGCAATCAAGTCGCCGCA
AGCCAGGGTTTTCGCTTTGGTCGCTGTGAGGCTCCGGGGCTATTTCGCTGGTATCCACTATGATGTCTC
GATGTGCAATTGATTGGGCGCGGTCTGTGAGGGCTCTTAGTGGCAAGCTGCCAAACCATGCAAGCATA
AAGCGGCGCCGGTCGCCTTTTTACGTGCAGTAAAAGCGCGCAGTGAGCGCTGTGACGCGTTCAGCTTG
CATCAATTCCTGACATAATCCTTCGCCTATCGCGTTCCCGCCCTGCCGTGCAGGTGCAGGCCT**tgtgtggaat**
tgtgagcggataacaatttcacacaggaaacagctatgaccatgattacgccaagcgcgcaattaaccctcactaaagggaacaaaagctgggtaccgggcc
ccccctcgagcacacacctgtcagaaacacgtctccgccacgctctccctctcacggccgaccccgcagccctttttgccctttcctaggccaccgacaggaccca
ggcgctctcagcatgcctcaacaacccgtactcgtgccagcggtgcccttgtgctggtgatcgcttggaagcgcatgcgaagacgaaggggcggagcaggcg
gcctggctgttcgaagggctcgccgccagttcgggtgccttttctccacgcgcgcctccacacctaccgatgcgtgaaggcaggcaaatgctcatgtttgcccga
actcggagtccttaaaaagccgcttcttgtcgtcgttccgagacatgttagcagatcgcagtgccacctttcctgacgcgctcggccccatattcggacgcaattg
tcatttgtagcacaattggagcaaatctggcgaggcagtaggcttttaagttgcaaggcgagagagcaaagtgggacgcggcgtgattattggtatttacgcga
cggcccggcgcgttagcggcccttccccaggccagggacgattatgtatcaatattgttgcgttcgggcactcgtgcgagggctcctgcgggctggggaggg
ggatctgggaattggaggtacgaccgagatggcttgctcgggggggaggtttcctcgccgagcaagccagggttaggtgttgcgctcttgactcgttgtgcattct
aggaccccactgctactcacaacaagcccatatggacgatgcgttgcgtgcactgcggggtcggtatcccggttgtgagtgggttgttgtggaggatggggcct
cgggggctggtgtttatcggcttcggggtggtgggcgggagttgtttgtcaaggtggcagctctgggggccggggtgggcttgttgggtgaggctgagcggctg
gtgtggttggcggaggtggggattcccgtacctcgtgttgtggagggtggtggggacgagagggtcgcctggttggtcaccgaagcggttccggggcgtccgg
ccagtgcgcggtggccgcgggagcagcggctggacgtggcggtggcgctcgcggggctcgctcgttcgctgcacgcgctggactgggagcggtgtccgttcg
atcgcagtctcgcggtgacggtgccgcaggcggcccgtgctgtcgctgaagggagcgtcgacttggaggatctggacgaggagcggaaggggtggtcgggg
gagcggcttctcgccgagctggagcggactcggcctgcggacgaggatctggcggtttgccacggtcacctgtgcccggacaacgtgctgctcgaccctcgta
cctgcgaggtgaccgggctgatcgacgtggggcgggtcggccgtgcggaccggcactccgatctcgcgctggtgctgcgcgagctggcccacgaggaggac
ccgtggttcgggccggagtgttccgcggcgttcctgcgggagtacgggcgcgggtgggatggggcggtatcggaggaaaagctggcgttttaccggctgttgg
acgagttcttctgagatatcgaattctcaggtcgggacatccccgaccaggggcggcggggatgttgctgggccgatggaaagGGTCGGCCCCGAC
GAGGCGCTGTTCGACGCCGTGGAGCGCTACGATGTGGACCTGCCCTACCTGTGCCGCACTGGTGAGAG
TTCGTGTGTTCGGCACACATACGCAGAAGCGTGGCACACACGGTTGTTGGGCAGCCCCGCTGCAAGTG
CACCAGTGCCCCTTACTCCCTTCCGACCCACATCCTGACCCTCCCCGCCCCTCCTCTCCTCCCCAACCCC
CAGGCACCTGCGGCACGTGCGCGGGCCGTGTGCAGGAGGGCCAGGTGGAGCTCAAGGGTCAGCACAT
CCTGGACCCCGATCAGGTCAAGGCCGGCTTCATCCTCATGTGCTCCGCCTACCCCCGCTCCGACTGCAC
CATCCTCACGCACCAGGTGAGGAGAGGGAAACAGGGATTGGAAAGAGATACGGCGCATCCGTGTGTG
CGGCTTGTGCGTGTGACCAGTGGTGCGGTGGCTGATGTGGGGTAAGGTGGGGTCGCGAAAGATGGAT
GCGATGGCCAGGGGTCGCTGCTGGGCTGCTGCTCGGAACGGCCTGCAACCGCACGTGCGTGTCCTTCG
GAGCCGCACCTGGCCGCGCCACACGTGCCTGTTTACTCCCAAGTCATTGACGCCTCCGCCCCCCCTGTG
CTCCCCGCCCCTTCCCTCCCCCTTCAGGAGGAGCGCCTGCACACCTGCGAGTACGGCAAGCACCAGTA
AGCGGCACACACACGCCGCACGTACCATTCGTGTCAGCGTCCGCTGCCTGGCGCCTGCTTGGAGCTAG
AGGCGGGCGATGGCGCAGTGGCACCAACATGACTCGTGACTCATAGGACAACATTGTTACTTTATCAC
GCAACGGAGGGGCATAGCTACGCTGGACAGGCTAGGCACGCACGACTCCTGCGCTGATTTGACTCCGT
AGGTAGATGAATGACTTCCACACAGTACCGGTATTGAACACCTTGACTCGCGCCTTGACGCATTGTTTT
GCCCGCACATATACGGGGCAGGAGTGGGTGGTGGTGCAAGCCGCCGCGCTCCGTGATTTTTGACGTTT
TGACACGCGGCTTGAAGAGTCAAGAGTGGCTGCAGCAGGATGCGAAGCATGTATGGCGGGGGTGACT
GAGGTAGGGCCGTAGAGGCAGGTTGACCGTTAGGCCTTAGGACGTCATGCATTGCCAAATGCCATACA
TGAGTGGGGCACGTGAGGATTGGTTGAGGATGGGACTGATTGAGGCACACATACCGTAGGCAGGTGA
TTATAATAACGGAGCGACTGCTCCTGGGTAGCGTGTGTGTGGCAAGGACACGGGTATGTATGGCTC
TGGTGTGGCTGAGTGCGGCGCCCCGCTAGCAAGCGGGGCTGCTGGAGGCGACTGGGTACCCGCGTGTC
TACTGCCGCAGAGAAGATTAAATCAAGCGATGAATTGGGTCACGGCTAGCTGCAAATGCAGCAGCTTC
ATGTAACCCCCAACTATGG

CDS sequence of *fdx5* mutant. The red uppercase letters represent the exons, and the lowercase letters represent the insertion cassette.

ATGCTGTGCGCGCGCTCCCAGCTGGTCTGCAAGCCTGTGAAGGCTGCTCGCGCCTCTCGCGCTACCGTC
AAGGTGCAGGCCT**tgtgtggaattgtgagcggataacaatttcacacaggaaacagctatgaccatgattacgccaagcgcgcaattaaccctcact**
aaagggaacaaaagctgggtaccgggccccccctcgagcacacacctgtcagaaacacgtctccgccacgctctccctctcacggccgaccccgcagcccttt
tgccctttcctaggccaccgacaggacccaggcgctctcagcatgcctcaacaacccgtactcgtgccagcggtgcccttgtgctggtgatcgcttggaagcgc
atgcgaagacgaaggggcggagcaggcggcctggctgttcgaagggctcgccgccagttcgggtgcctttctccacgcgcgcctccacacctaccgatgcgtg
aaggcaggcaaatgctcatgtttgcccgaactcggagtccttaaaaagccgcttcttgtcgtcgttccgagacatgttagcagatcgcagtgccacctttcctga
cgcgctcggccccatattcggacgcaattgtcatttgtagcacaattggagcaaatctggcgaggcagtaggcttttaagttgcaaggcgagagagcaaagtg
gacgcggcgtgattattggtatttacgcgacggcccggcgcgttagcggcccttcccccaggccagggacgattatgtatcaatattgttgcgttcgggcactc
gtgcgagggctcctgcgggctggggaggggatctgggaattggaggtacgaccgagatggcttgctcgggggggaggtttcctcgccgagcaagccagggtt
aggtgttgcgctcttgactcgttgtgcattctaggaccccactgctactcacaacaagcccatatggacgatgcgttgcgtgcactgcggggtcggtatcccggtt
gtgagtgggttgttgtggaggatggggcctcgggggctggtgtttatcggcttcggggtggtgggcgggagttgtttgtcaaggtggcagctctgggggccggg
gtgggcttgttgggtgaggctgagcggctggtgtggttggcggaggtggggattcccgtacctcgtgttgtggagggtggtggggacgagagggtcgcctggtt
ggtcaccgaagcggttccggggcgtccggccagtgcgcggtggccgcgggagcagcggctggacgtggcggtggcgctcgcggggctcgctcgttcgctgca
cgcgctggactgggagcggtgtccgttcgatcgcagtctcgcggtgacggtgccgcaggcggcccgtgctgtcgctgaagggagcgtcgacttggaggatctg
gacgaggagcggaaggggtggtcgggggagcggcttctcgccgagctggagcggactcggcctgcggacgaggatctggcggtttgccacggtcacctgtg
cccggacaacgtgctgctcgaccctcgtacctgcgaggtgaccgggctgatcgacgtggggcgggtcggccgtgcggaccggcactccgatctcgcgctggtg
ctgcgcgagctggcccacgaggaggacccgtggttcgggccggagtgttccgcggcgttcctgcgggagtacgggcgcgggtgggatggggcggtatcgga
ggaaaagctggcgttttaccggctgttggacgagttcttctgagatatcgaattctcaggtcgggacatccccgaccaggggcggcggggatgttgctgggccg
atggaaagGGTCGGCCCCGACGAGGCGCTGTTCGACGCCGTGGAGCGCTACGATGTGGACCTGCCCTACC
TGTGCCGCACTGGCACCTGCGGCACGTGCGCGGGCCGTGTGCAGGAGGGCCAGGTGGAGCTCAAGGG
TCAGCACATCCTGGACCCCGATCAGGTCAAGGCCGGCTTCATCCTCATGTGCTCCGCCTACCCCCGCTC
CGACTGCACCATCCTCACGCACCAGGAGGAGCGCCTGCACACCTGCGAGTACGGCAAGCACCAGTAA